International Journal of Modern Physics B
Vol. 27, No. 30 (2013) 1350174 (10 pages)

DOI: 10.1142/S0217979213501749

EFFECT OF HEAT TREATMENT ON MICROSTRUCTURE AND MAGNETOSTRICTIVE PROPERTY OF MELT-SPUN $Fe_{85}Ga_{15}$ RIBBONS

HAO LIU, HAIOU WANG, MENGXIONG CAO and WEISHI TAN*

Department of Applied Physics,
Nanjing University of Science and Technology,
Nanjing, 210094, P. R. China
**tanweishi@njust.edu.cn*

YANGGUANG SHI

Department of Applied Physics,
Nanjing University of Aeronautics and Astronautics,
Nanjing, 211106, P. R. China

YU CHEN

Institute of High Energy Physics, Chinese Academy of Sciences,
Beijing, 100039, P. R. China

YUYING HUANG

Shanghai Institute of Applied Physics, Chinese Academy of Sciences,
Shanghai, 201800, P. R. China

Received 1 May 2013
Revised 31 July 2013
Accepted 28 August 2013
Published 18 September 2013

In order to study the microstructure of Fe–Ga alloy, $Fe_{85}Ga_{15}$ ribbons prepared with different wheel velocity were studied by high resolution X-ray diffraction (HRXRD) and extend X-ray absorption fine structure (EXAFS). HRXRD patterns showed that only disordered A_2 phase was observed in as-cast $Fe_{85}Ga_{15}$ alloy. A modified-DO_3 phase was detected in all of the melt spun samples. The HRXRD associated with EXAFS results indicated that Ga atoms were located as second-nearest neighbor along [100] orientation. A little DO_3 phase was found in ribbons annealed at 1000°C under 0.06 MPa Ar atmosphere. The result of magnetostriction measurement revealed that in the ribbon prepared with higher wheel velocity, more modified-DO_3 phase will enhance the magnetostriction. DO_3 phase in the annealed sample will deteriorate the magnetostrictive properties of Fe–Ga ribbons.

*Corresponding author.

Keywords: HRXRD; EXAFS; modified-DO_3 phase; magnetostriction; Fe–Ga ribbon.

PACS numbers: 61.50.Ks, 75.50.Bb

1. Introduction

Fe–Ga alloy is a new magnetostrictive material of lower price and better extensibility in comparison with conventional Tb–Dy–Fe alloys. Many researches revealed that the microstructure and magnetostriction are influenced strongly by preparing method and heat treatment.[1,2] In Fe–Ga alloys A_2, DO_3, $L1_2$, B_2, DO_{19} and modified-DO_3 (B_2 like) phase appeared with different preparing methods.[3–5] Early works on theoretical simulations showed that the magnetostrictive coefficients strongly depend on the atomic arrangement and an unstable modified-DO_3 structure plays a positive role in the magnetostriction.[6] Cullen *et al.* proposed that a short range ordering (SRO) of Ga atoms cluster along [100] direction acted as locally distorted anisotropic defects.[7] These atom clusters can change their orientations under application of magnetic field and therefore increase the magnetostriction. Although theoretically research predicted that a modified-DO_3 phase should be the main reason of large magnetostriction in Fe–Ga alloys, there is no sufficient evidence to confirm this prediction. Recently, many researches about Fe–Ga alloys attributed a diffraction peak split of A_2 phase in X-ray diffraction (XRD) patterns to modified-DO_3 phase.[5,8] In fact, it is difficult to distinguish modified-DO_3 phase from other phase because, other than modified-DO_3 phase, diffraction peaks of both DO_3 phase and B_2 phase will overlap with the main peaks of A_2 matrix. Moreover, the small difference between the atomic scattering factors of Fe and Ga in this system results in extremely weak superlattice reflections, which made it difficult to distinguish the ordered phases using conventional XRD. To test and verify the theoretical calculation, it is necessary to detect the modified-DO_3 phase in experiment with higher resolution. Synchrotron radiation resource is of high intensity and high resolution and can help us to detect many weak diffraction peaks and identify the ordered phase. Furthermore, a distorted DO_3 phase was found to bring a local stress and lead to an enhancement of magnetoelastic effect and a giant magnetostriction.[9] An SRO DO_3 phase was found in Fe–Ga single crystal, and X-ray diffuse scattering measurement illustrated that the SRO DO_3 phase plays a negative role in the magnetostriction.[10,11] Liu *et al.* also indicated that the ordered DO_3 phase is harmful to the improvement of magnetostriction.[12] From the above, whether DO_3 phase in FeGa alloy was beneficial to the magnetostriction or not was controversial, thus more experimental data, especially information on the local structure, was necessary to point out the arrangement of Ga atoms and its influence on the magnetostriction in Fe–Ga alloy.

Accordingly, the purpose of this study is to characterize the microstructure of Fe–Ga alloys in detail and to investigate the influence of heat treatment on the microstructure and magnetostriction. Based on this purpose, we utilized high resolution X-ray diffraction (HRXRD) to characterize the phase structure and used

extended X-ray absorption fine structure (EXAFS) to study the local structure of the ribbons in Synchrotron Radiation Facility. The results of HRXRD and EXAFS were employed to reveal the distribution mode of Ga atoms. Whether modified-DO_3 phase existed in our samples was talked about. The relation between microstructure and magnetism, magnetostriction was discussed.

2. Experimental Procedure

Pure gallium (99.999%) and pure iron (99.99%) were cleaned and arc melted together several times with composition of $Fe_{85}Ga_{15}$ under argon atmosphere. The as-cast ingot was crushed into small pieces of mass about 5 g, which were then melt spun to ribbons using linear velocities of a copper wheel of 12.5 m/s and 25 m/s. The as-quenched ribbons were of the width 2–3 mm and thickness of 50–100 μm. The ribbon prepared with wheel velocity of 12.5 m/s was annealed at 1000°C under 0.06 MPa argon atmosphere for 10 h and then cooled to room temperature at 5°C/min. To describe conveniently, we named ribbons prepared with 12.5 m/s and 25 m/s wheel velocity as $S_{12.5}$ and S_{25}, respectively.

In order to observe the weak diffraction peaks which are difficult to be recognized in conventional XRD patterns, our HRXRD patterns were obtained in beam line 1W1A of Beijing Synchrotron Radiation Facility (BSRF). The wavelength is 0.15405 nm. Fluorescence EXAFS of Fe K-edge and Ga K-edge were measured in beam line BL14W of Shanghai Synchrotron Radiation Facility (SSRF) to probe the local structure of the ribbons. Self-absorption calibration was considered to reduce simulation errors resulting from high concentration of Fe and Ga. The magnetization curves of our samples were measured using vibrating sample magnetometer (VSM), and the direction of magnetic field was along the ribbon length. The magnetostriction coefficients of the ribbons were measured using strain gauge. To avoid the bending of ribbon in magnetic field, we glued about 20 ribbons together. The magnetostriction was measured with applied magnetic field along the ribbon length direction and the ribbon normal direction.

3. Results and Discussion

The HRXRD patterns of samples, shown in Fig. 1(a), illustrated that there was only disordered A_2 phase in the as-cast alloy. Figure 1(b) showed the enlarged patterns of Fig. 1(a). We noted that a diffraction peak appeared at about 21.8° in the HRXRD patterns of sample $S_{12.5}$. Many diffraction peaks emerged around 21.8°, 31.0°, 38.2° and 60.0° after annealing at 1000°C. For the sample S_{25}, there were three weak diffraction peaks around 21.8°, 31.0° and 38.2°. By comparing these diffraction patterns with calculated patterns of some possible phase with the known lattice constant before, we found that these diffraction peaks came from modified-DO_3 phase proposed by Lograsso.[4] Calculated pattern of modified-DO_3 phase was also shown at the bottom of Fig. 1(b). We found that diffraction peaks were fitted well. The peak at 21.8° was (100) diffraction peak of modified-DO_3 phase. In the HRXRD

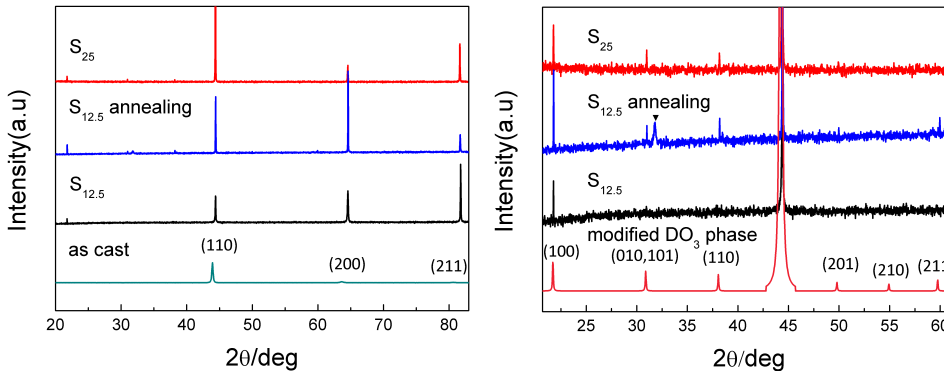

Fig. 1. (a) HRXRD patterns of as-cast alloy and $Fe_{85}Ga_{15}$ ribbons prepared with different wheel velocity and heat treatment, (b) simulated XRD patterns of modified-DO_3 phase and enlarged experimental XRD patterns.

pattern of $S_{12.5}$ sample, only (100) peak of modified-DO_3 phase was detected. This can be explained as follows: $S_{12.5}$ sample was of strong (100) texture despite the fact that there was lower amount of modified-DO_3 phase in $S_{12.5}$ sample than that in S_{25} sample, therefore, $S_{12.5}$ sample presented high intensity at 21.8°. More experimental data about modified-DO_3 will be shown below. For the sample annealed at 1000°C, there was a specific peak around 31.0° (marked with ▼), which may originate from an order DO_3 phase.

The work of Xing *et al.*[13] indicated that for the single crystal Fe–Ga alloy, the single-phase A_2 structure can be retained up to 17.9 at.% Ga with slow-cooling process and up to 21.2 at.% Ga with quenching. In our experiment, an additional modified-DO_3 phase precipitated in 15 at.% Ga. This phenomenon stated that the additional phase was easier to form in melt-spun ribbons than in single crystal.

The lattice constant of A_2 and modified-DO_3 phase and grain size were calculated by Bragg equation and Scherrer's equation, respectively. The grain size was estimated after the measured width of (200) peaks in XRD pattern was calibrated by taking out width contribution resulting from diffractometer. The lattice constants and grain size are presented in Table 1. The results in Table 1 indicate that lattice constant of as-quenched ribbons is smaller than that of as-cast alloy. The lattice constant of S_{25} is larger than that of $S_{12.5}$. Annealing procedure reduced the lattice constant in $S_{12.5}$. The result of lattice constants indicated that the heat treatment changed the cell size. From Table 1, we found that half of $a_{\text{modified-DO}_3}$ was close to lattice constant a_{A_2}. For instance, a_{A_2} of S_{25} was 0.28843 nm, which was close to half of $a_{\text{modified-DO}_3}$ 0.28849 nm. In addition, a_{A_2} reduced from 0.28843 nm to 0.28833 nm with decrease of the wheel velocity; on the other hand, $a_{\text{modified-DO}_3}$ increased from 0.57699 nm to 0.57704 nm. The ribbons were of larger grain size than that of as-cast alloy. Higher wheel velocity resulted in larger grain size of about

Table 1. Lattice constant and grain size of $Fe_{85}Ga_{15}$ prepared with different wheel velocity and heat treatment.

	Lattice constant of A_2 matrix (nm)	Lattice constant of modified DO_3 (nm)	Grain size (nm)
as cast	0.29124		15
$S_{12.5}$	0.28833	0.57704	65
S_{25}	0.28843	0.57699	95
$S_{12.5}$ annealing	0.28826	0.57649	140

95 nm and the grain size increased to about 140 nm after annealing. In other words, both the increasing of wheel velocity and annealing can increase the grain size.

HRXRD is only sensitive to long range ordering (LRO) but cannot be used to detect the local structure. To characterize the local structure and the atom arrangement in our ribbons, we measured Fe K-edge and Ga K-edge absorption spectrum of S_{25}. The EXAFS oscillations were extracted from the experimental date using standard procedures. At first, self-absorption calibration was carried out to avoid the effect of high concentration of absorption elements in fluorescence mode. Then the pre-edge background was subtracted with a linear function while R_{bkg} parameter was equal to 1.2.

The experimental χ_k functions for Fe and Ga K-edge are shown in Fig. 2. The Fourier transformation (FT) was calculated using the Hanning filtering function. To enhance the oscillations at higher k, the k^2 weighted data were used. The FT was performed in the range 30 $nm^{-1} < k < 144$ nm^{-1}. The lattice parameter ($a = 0.28843$ nm) previously obtained by HRXRD data indicated that there were two coordination shells between 0.1 nm $< R <$ 0.3 nm, but the proximity of the two neighboring shells and the limited R-space resolution do not allow us to resolve these two shells, so the fitting procedure was used to obtain the coordination information of the first two shells.

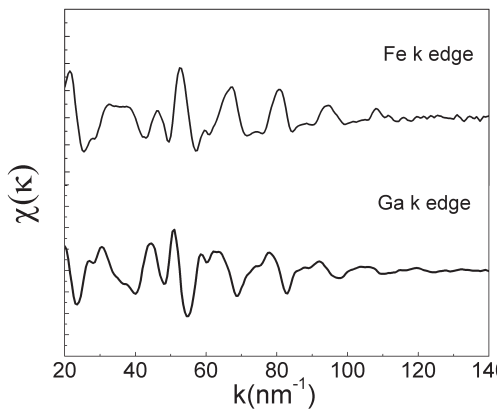

Fig. 2. Experimental χ_k functions for investigated S_{25} and measured for Fe and Ga K-edge.

In this study, Fe and Ga K-edge extended X-ray absorption fine structure spectrum of S_{25} and were fitted simultaneously by FEFFIT.[14] Fitting strategy of Pascarelli[15] was adopted in our work. In order to reduce the variables, many relations between different fitting parameters were set. Fitting parameters were set as follows: for both Fe and Ga atom, there were eight atoms in the first shell and six atoms in the second shell around the absorption atom due to bcc structure. For Fe K-edge data, the chemical composition of the first shell was defined as $x = N_{\mathrm{FeGa}}/(N_{\mathrm{FeFe}} + N_{\mathrm{FeGa}})$, here N_{FeFe} and N_{FeGa} represented the number of Fe atoms and Ga atoms in the first shell around Fe atom, respectively. Ga atom in the second shell was tested in another way in the following. E_0 offset of Fe and Ga was ΔE_1 and ΔE_2, respectively. We defined the average relative atomic displacements with respect to crystallographic distance, $\alpha = \Delta R/R$. For example, α_{FeGa} means the average relative displacements of Ga atom around Fe atom with respect to crystallographic distance. Taking into account the crystallization condition of iron-based alloy, $R^{\mathrm{II}} = (2/\sqrt{3})R^{\mathrm{I}}$ (the superscript I and II represent the first and the second shell, respectively), we fixed $\alpha^{\mathrm{I}}_{\mathrm{FeFe}} = \alpha^{\mathrm{II}}_{\mathrm{FeFe}}$. Considering that the first coordination shell would bring larger lattice relaxation,[16] we performed the simulation by changing the value of $\alpha^{\mathrm{I}}_{\mathrm{FeGa}}$, $\alpha^{\mathrm{I}}_{\mathrm{GaFe}}$, $\alpha^{\mathrm{II}}_{\mathrm{FeGa}}$, $\alpha^{\mathrm{II}}_{\mathrm{GaFe}}$, $\alpha^{\mathrm{I}}_{\mathrm{GaGa}}$ and $\alpha^{\mathrm{II}}_{\mathrm{GaGa}}$ under the conditions of $\alpha^{\mathrm{I}}_{\mathrm{GaFe}} = \alpha^{\mathrm{I}}_{\mathrm{FeGa}}$, $\alpha^{\mathrm{II}}_{\mathrm{FeGa}} = \alpha^{\mathrm{II}}_{\mathrm{GaFe}}$. The disordered parameters were labeled as $(\sigma^2)^{\mathrm{I}}_{\mathrm{FeFe}}$ and $(\sigma^2)^{\mathrm{II}}_{\mathrm{FeFe}}$ for the Fe–Fe pairs, and $(\sigma^2)^{\mathrm{I}}_{\mathrm{FeGa}} = (\sigma^2)^{\mathrm{I}}_{\mathrm{GaFe}}$, $(\sigma^2)^{\mathrm{II}}_{\mathrm{FeGa}} = (\sigma^2)^{\mathrm{II}}_{\mathrm{GaFe}}$ for the Fe–Ga pairs, and $(\sigma^2)^{\mathrm{I}}_{\mathrm{GaGa}}$, $(\sigma^2)^{\mathrm{II}}_{\mathrm{GaGa}}$ for the Ga–Ga pairs. The amplitude damping factor S_0^2 was fixed to be 0.7.

We used different models by progressively substituting Fe with Ga atoms around Fe and Ga atoms. The suitability of each model was evaluated by comparing reduced χ square variables, χ^2_ν. For the Fe K-edge data, substituting one Fe atom with one Ga in the second shell did not change the value of χ^2_ν, so that we had no sensitivity to test the Ga atoms in the second shell around Fe. For the Ga K-edge data, when we substituted Fe with Ga in the first shell, the value of χ^2_ν increased sharply. When we substituted one Fe atom with one Ga atom in the second shell, the value of χ^2_ν decreased about 40%. One more Ga atom substitution caused χ^2_ν reduction of 10%. Continuous substitution of the Ga atom led to an increase of χ^2_ν about 10%, as shown in Fig. 3. The most reasonable fitting results correspond to the minimum of χ^2_ν. Fitting results implied that there was no Ga atom in the first coordination shell and there were two Ga atoms in the second coordination shell around Ga atom.

The results of the EXAFS were in accordance with the modified-DO_3 phase obtained by HRXRD because there were two Ga atoms in the second coordination shell around Ga atom in modified-DO_3 phase. The best fitting results are shown in Fig. 4. It fitted well at the first peak of R space.

The structure parameter of the best fitting is shown in Tables 2 and 3. The content of Ga atoms in the first shell of Fe was 0.27, which was slightly higher than that for the case of random distribution, indicating that there may exist a Ga cluster. The obtained value of the Fe–Ga bond is 0.251 nm whereas the Fe–Fe bond is 0.247 nm, implying lattice expansion of about +4%. In the second shell,

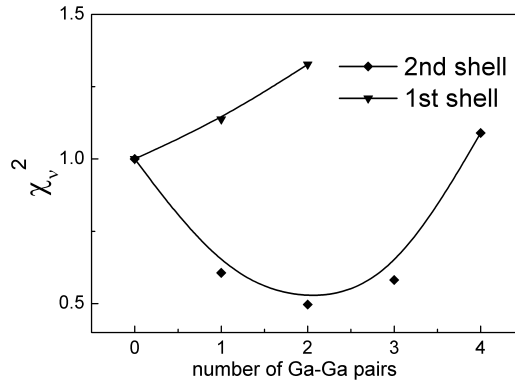

Fig. 3. Normalized χ_ν^2, obtained for the simultaneous Fe and Ga K-edge fitting of S_{25} with different structure model.

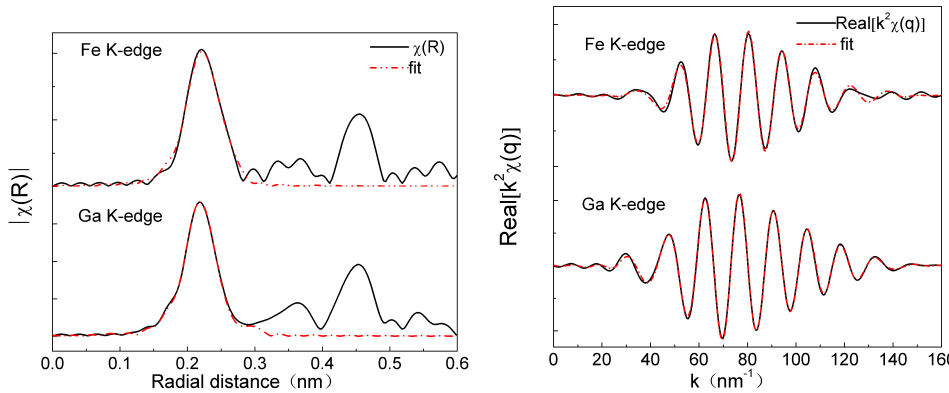

Fig. 4. Fitting curves in (a) R space and (b) k space of Fe and Ga K-edge EXAFS of S_{25}.

Table 2. The best fitting structural parameters of Fe K-edge.

x	$R^{\mathrm{I}}_{\mathrm{FeFe}}$ (nm)	$R^{\mathrm{II}}_{\mathrm{FeFe}}$ (nm)	$(\sigma^2)^{\mathrm{I}}_{\mathrm{FeFe}}$ (nm^2)	$(\sigma^2)^{\mathrm{II}}_{\mathrm{FeFe}}$ (nm^2)	ΔE_1 (eV)
0.27	0.247 ± 0.001	0.285 ± 0.001	4×10^{-5}	6×10^{-5}	1.8

Table 3. The best fitting structural parameters of Ga K-edge.

$R^{\mathrm{I}}_{\mathrm{GaFe}}$ (nm)	$R^{\mathrm{II}}_{\mathrm{GaFe}}$ (nm)	$R^{\mathrm{II}}_{\mathrm{GaGa}}$ (nm)	$(\sigma^2)^{\mathrm{I}}_{\mathrm{GaFe}}$ (nm^2)	$(\sigma^2)^{\mathrm{II}}_{\mathrm{GaFe}}$ (nm^2)	$(\sigma^2)^{\mathrm{II}}_{\mathrm{GaGa}}$ (nm^2)	ΔE_2 (eV)
0.251 ± 0.001	0.287 ± 0.001	0.305 ± 0.003	5×10^{-5}	4×10^{-5}	7×10^{-5}	9.2

strain quickly relaxed down to +0.7%, since we found Fe–Ga bonds of 0.287 nm and Fe–Fe bonds of 0.285 nm. On the other hand, in the second shell, Ga–Ga bond distance is highly larger (0.305 nm) than the corresponding Fe–Fe distance of the host lattice (0.285 nm).

Figure 5(a) shows the magnetization curves of $Fe_{85}Ga_{15}$ alloys. In the experiment the magnetic field was applied along the ribbon length direction. The inset of Fig. 5(a) shows enlarged magnetization curves with the applied magnetic field ranging from 0.1 T to 0.9 T. The saturation magnetization (Ms) of as-cast alloys, $S_{12.5}$ and S_{25} were determined to be 163.57, 172.76 and 173.01 emu/g, respectively. The value of Ms reached to 174.5 emu/g when $S_{12.5}$ was annealed in Ar atmosphere for 10 h. We found that the values of Ms depended on the grain size, i.e., the value of Ms increased with increasing grain size. Although the value of Ms of $S_{12.5}$ and S_{25} were almost identical, it is more difficult for S_{25} to saturate along the ribbon

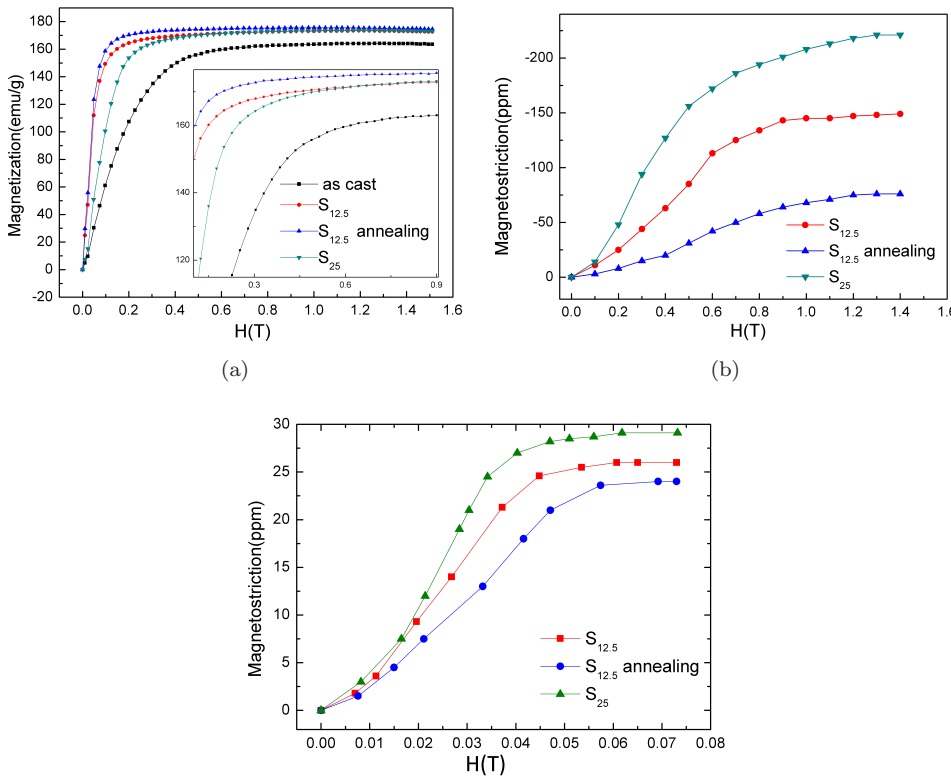

Fig. 5. (a) Magnetization curves of $Fe_{85}Ga_{15}$ as-cast alloy, ribbons and annealing sample at 1000°C. The magnetic field was applied along the ribbon length direction. The inset was the enlarged magnetization curves. (b) Magnetostriction of $Fe_{85}Ga_{15}$ ribbons and annealing sample at 1000°C. The magnetic field was (b) along the ribbon normal direction and (c) along the ribbon length direction.

length direction. The saturation magnetic field of $S_{12.5}$ annealed at 1000°C, $S_{12.5}$ and S_{25} were estimated to be about 0.18, 0.26 and 0.4 T, respectively. The difference of saturation magnetic field between these samples could be explained from different lattice orientation in three ribbons.

The magnetostriction of $Fe_{85}Ga_{15}$ alloy are presented in Figs. 5(b) and 5(c). When the magnetic field was applied along the normal of the ribbons, the saturation magnetostriction of $S_{12.5}$ reached to −149 ppm, which decreased to −76 ppm after annealing in Ar atmosphere at 1000°C for 10 h and increased to −221 ppm in S_{25}. When the magnetic field was applied along the ribbon length direction, the saturation magnetostriction of $S_{12.5}$, annealed $S_{12.5}$ and S_{25} was 26, 24 and 29 ppm, respectively. Considering the magnetic curves measured previously, we found that the saturation magnetostriction of ribbons increased with increasing saturation magnetic field.

During the melt spinning process, the alloy can no longer maintain disordered A_2 phase, and one part of A_2 phase transformed to modified-DO_3 superlattice structure by adjusting Ga atoms to distribute along [100] orientation due to temperature gradient. For $S_{12.5}$, there was only one characteristic diffraction peak of modified-DO_3 phase around 21.8° in HRXRD pattern, whereas there were many diffraction peaks in S_{25}. The result indicated that higher wheel velocity introduced more modified-DO_3 phase, that is, more Ga–Ga atom pairs along [100] orientation emerged. These pairs created a local stress which will couple with external strain and therefore soften the modulus. It results in an enhancement of magnetoelastic effect and an improved magnetostriction, as described in the investigations on Fe–Ga alloys.[17] However, no split of diffraction peak was detected since the difference of the lattice constant between modified-DO_3 phase and A_2 matrix was very small. In addition, various heat treatments induced different lattice orientation during melt spinning process. The lattice orientation also played an important role in the magnetic properties.

After annealing, besides modified-DO_3 phase, a little DO_3 phase precipitated in the ribbon because of recrystallization. In the DO_3 phase, Ga atoms arranged along the [110] orientation. This kind of arrangement of Ga atoms played a negative role in the improvement of magnetostriction, and therefore, magnetostriction of FeGa ribbons decreased after annealing.

4. Conclusion

Our research indicated that the heat treatment affects the structure of the $Fe_{85}Ga_{15}$ ribbons obviously. Heat treatment transformed one part of the disordered A_2 phase into an ordered DO_3 phase and an modified-DO_3 phase and decreased the lattice constants. We clarified that the modified-DO_3 phase, in which Ga–Ga atom pairs distribute along [100] orientation, is beneficial to the increasing of the magnetostriction. High wheel velocity resulted in generation of more modified-DO_3 phase, thus S_{25} is of the highest magnetostriction coefficient of −221 ppm in all our samples.

Annealed sample presented a smaller magnetostriction of −76 ppm mainly due to formation of ordered DO_3 phase, in which the Ga–Ga pairs arrange along [110] orientation. In addition, lattice orientation played an important role in the magnetic property of the ribbons.

Acknowledgments

We acknowledge the help from colleagues at the Shanghai Synchrotron Radiation Facility (SSRF) and Beijing Synchrotron Radiation Facility (BSRF). The study was supported by Natural Science Foundation of China with Grant No. 11079022.

References

1. S. Guruswamy *et al.*, *Scri. Mater.* **43**, 239 (2000).
2. A. E. Clark *et al.*, *IEEE Trans. Magn.* **37**, 2678 (2001).
3. N. Srisukhumbowornchai and S. Guruswamy, *J. Appl. Phys.* **92**, 5371 (2002).
4. T. A. Lograsso *et al.*, *J. Alloys. Compd.* **350**, 95 (2003).
5. G. D. Liu *et al.*, *Appl. Phys. Lett.* **84**(12), 2124 (2004).
6. R. Wu, *J. Appl. Phys.* **91**, 7358 (2002).
7. J. Cullen, P. Zhao and M. Wuttig, *J. Appl. Phys.* **101**, 123922 (2007).
8. J. Liu, F. Yi and C. Jiang, *J. Alloys. Compd.* **481**, 57 (2009).
9. M. C. Zhang *et al.*, *J. Appl. Phys.* **99**, 023903 (2006).
10. M. Huang and T. A. Lograsso, *Appl. Phys. Lett.* **95**, 171907 (2009).
11. Y. Du *et al.*, *Phys. Rev. B* **81**, 054432 (2010).
12. G. D. Liu *et al.*, *J. Appl. Phys.* **99**, 093904 (2006).
13. Q. Xing *et al.*, *Acta Mater.* **56**, 4536 (2008).
14. M. Newville, *J. Synchrotron Rad.* **8**, 322 (2001).
15. S. Pascarelli *et al.*, *Phys. Rev. B* **77**, 184406 (2008).
16. U. Scheuer and B. Lengeler, *Phys. Rev. B* **44**, 9883 (1991).
17. M. Wutting, L. Dai and J. Cullen, *Appl. Phys. Lett.* **80**, 1135 (2002).